materials proceedings

MDPI

Proceeding Paper

Biosynthesis of Titanium Dioxide Nanoparticles by the Aqueous Extract of *Juglans regia* Green Husk †

Zahra Heydari and Parinaz Ghadam *

Department of Biotechnology, Faculty of Biological Sciences, Alzahra University, Tehran 1993893973, Iran; heydarizahra57@yahoo.com

* Correspondence: pghadam@alzahra.ac.ir

† Presented at the 4th International Online Conference on Nanomaterials, 5–19 May 2023; Available online: https://iocn2023.sciforum.net.

Abstract: A straightforward, non-toxic, economical, and environmentally safe method for nanoparticle (NP) synthesis is NP biosynthesis. An aqueous extract of the green husk of *Juglans regia* (*J. regia*) was used to produce titanium dioxide NPs (TiO_2 NPs) in this study. The green husk of walnuts is an agricultural waste that may contain valuable compounds. Numerous studies have demonstrated the potential of this inexpensive natural material as a source of phenolic compounds with antiradical and antimicrobial properties. The NPs were characterized using UV-Vis spectroscopy, X-ray diffraction, FT–IR spectroscopy, DLS, and FE-SEM. The UV–Vis spectrum displayed a significant peak at 334 nm. The as-fabricated TiO_2 NPs had two distinct phases that ranged in size from 19 to 23 nm on average. FT-IR analysis revealed the Ti-O bond. FE-SEM and EDX were used to characterize the spherical surface morphology and the Ti and O elemental configuration of the NPs, respectively. TiO_2 NPs are viewed as incredibly important nanomaterials as a result of their security, high strength, and photocatalytic properties. Accordingly, TiO_2 NPs are valuable in beauty-care products, substance detection, wastewater treatment, antimicrobial applications, hydrogen creation, and lithium-ion batteries.

Keywords: biosynthesis; green synthesis; titanium dioxide; *Juglans regia* green husk; anatase

Citation: Heydari, Z.; Ghadam, P. Biosynthesis of Titanium Dioxide Nanoparticles by the Aqueous Extract of *Juglans regia* Green Husk. *Mater. Proc.* **2023**, *14*, 43. https://doi.org/10.3390/IOCN2023-14482

Academic Editor: José Luis Arias Mediano

Published: 5 May 2023

1. Introduction

Nanotechnology is a rapidly expanding field in science and innovation. The creation or synthesis of nanomaterials, known as nanomaterials, is the science behind nanotechnology [1]. Organic and inorganic materials are the two types of nanomaterials that fall within the size range of 1–100 nm [2,3]. Biological, physical, and chemical methods are used to create nanomaterials. Bio-based protocols for the synthesis of NPs, also known as green synthesis, are simple, inexpensive, and suitable for larger-scale production [2,4]. The synthesis of NPs using biological agents has received a lot of attention in the nanotechnology field over recent decades [4].

TiO_2 NPs are regarded as one of the most valuable NPs because they are non-toxic, chemically and thermally stable, inexpensive, and photo-catalytically active [5,6]. There are three distinct polymorphs of binary metal oxides, each of which has a crystalline structure: brookite, rutile, and anatase. Rutile TiO_2 has a bandgap energy of 3.0 eV, anatase TiO_2 has a bandgap energy of 3.2 eV, and brookite TiO_2 has a bandgap energy of 3.2 eV. Self-cleaning solar cells, chemical sensors, gas sensors, anti-fogging and antimicrobial agents, deodorization, wastewater treatment, cosmetics, hydrogen production, and lithium-ion batteries are just a few of the many fields in which TiO_2 has received significant attention in recent decades [1,5,6]. Photocatalysis is thought to be the most useful of these because it uses sunlight to break down organic pollutants [5]. In this study, we have reported TiO_2 biosynthesis using an aqueous solution of the *J. regia* green husk.

2. Materials and Methods

2.1. Materials

The titanium tetraisopropoxide (TTIP, $Ti(OC_3H_7)_4$, purity $\geq$ 98 percent) was supplied by MERCK KGaA, Germany. The green husk was obtained from Iran's Zanjan region. During the process of making the leaf extract, distilled water and filter papers from Whatman, England, with pores measuring 1.2 µm, were used. The NPs were synthesized using deionized water as the solvent, and all other reagents were used as supplied without further processing.

2.2. Synthesis Method

Preparation of *J. regia* Green Husk Powder

After drying the *J. regia* green husk, 0.4 g of the powder was broken up in 15 mL of refined water and warmed at 100 °C in a bain-marie water bath for 10 min. The extract was made after filtering the yellowish solution with filter papers.

2.3. TiO_2NP Production

A total of 50 µL of TTIP was blended in with 0.5 mL of plant extract and 4.5 mL refined water was added twice to fabricate the G-TiO_2 NPs. The consolidated arrangement was blended for 24 h at ambient temperature. The yellowish solid was shaped and its presence was proof of NP formation. The solid was centrifuged at 5304× *g* for 10 min and washed multiple times. The as-fabricated NPs were grounded and calcined at 600 °C in a stifle heater for 4 h [6]. The prepared TiO_2 NPs were stored for further analysis.

2.4. Characterization of TiO_2 NPs

UV–Vis spectra were obtained with a Shimadzu UV-1800 spectrophotometer (Shimadzu Company, Kyoto, Japan) with a frequency range of 200–800 nm. The ordering and state of the translucent material were examined by X-ray diffraction investigation utilizing a Rigaku Ultima IV diffractometer (Tokyo, Japan). The functional groups and metal content were determined by FT-IR spectroscopy in the conveyance mode in a range of 4000–400 cm^{-1} using a TENSON 27 spectrometer (BRUKER, Karlsruhe, Germany). The hydrodynamic diameter of the biosynthesized TiO_2 NPs was determined using a VASCO TM particle size analyzer (CORDOUAN Innovation, Pessac, France). The morphology and size of the NPs and remaining components were examined by FESEM and EDX utilizing a MIRA3 microscope (TESCAN, Brno, Czech Republic). An electric stifle heater was utilized for the calcination of the TiO_2 NPs (Azar Heaters, Tehran, Iran).

3. Results and Discussion

3.1. UV—Vis Analysis

The Surface Plasmon Resonance (SPR) spectrum of the TiO_2 NPs revealed a maximum absorbance in the 300–350 nm range, indicating that colloidal titanium and titanium ions had exchanged (Figure 1) [7].

Equation (1) was used to calculate the TiO_2 NPs' energy band gap.

$$Eg = hc/\lambda \quad (1)$$

where h is the Planck Constant (4.135 × 10^{-15} eV·s); λ is the wavelength (in nm); and c is the speed of light (3 × 10^8 ms^{-1}) [8]. The absorption peak is located at a wavelength of 338 nm, and thus, the band gap was calculated to be 3.67 eV.

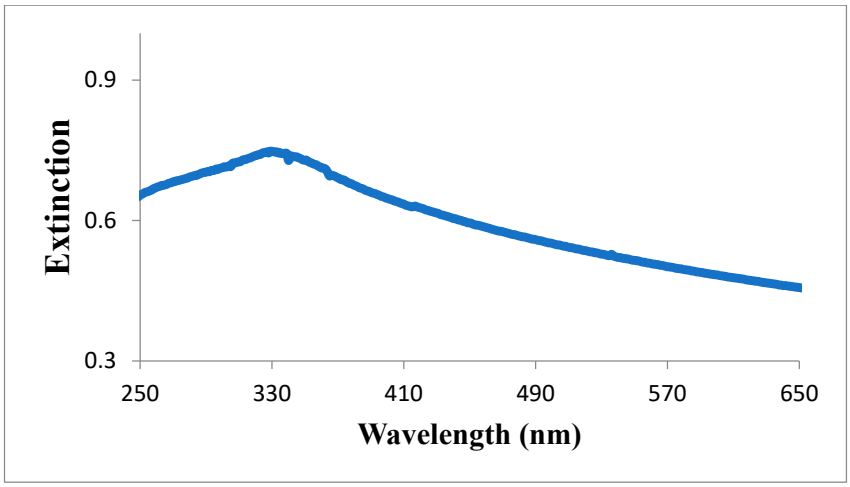

Figure 1. UV–Vis spectrum of the synthesized TiO_2 NPs.

3.2. XRD Analysis

X-ray diffraction (XRD) was used to determine the crystallinity of the NPs (Figure 2). The pattern confirms that the biosynthesized TiO_2 NPs are crystalline. The XRD pattern shows eight strong, broad peaks across the entire 2θ range with prominent peaks at 25.29°, 37.98°, 47.98°, 53.99°, 55.02°, 62.65°, 70.43°, and 73.3° attributed to the (101), (004), (200), (211), (211), (002), (220), and (215) crystal planes, respectively. The pattern also shows that the material is a mixture of anatase and rutile. The major plane of anatase is observed to be the plane (101) while the major plane of rutile is observed to be the plane (211). These findings are consistent with ICDD file Nos. 01-083-2243 (Anatase) and 00-004-0551 (rutile) [9]. The major peak at 25.29° in the XRD pattern of the synthesized NPs corresponds to the TiO_2 anatase (101) crystallographic plane. Using Debye–Scherrer's Equation (Equation (2)), the average crystallite size of the TiO_2 NPs was determined from the XRD pattern [10]:

$$D = K\lambda/(\beta \cos \theta) \quad (2)$$

where K is the shape factor (0.89); λ is the wavelength of X-ray radiation (0.15418 nm); β is the full width at half maximum (FWHM) of the diffraction peak of the crystallographic plane of anatase; and θ is the angle of the X-ray diffraction peak. The estimated and calculated sizes of the crystallites are presented in Table 1. The average crystallite size was found to be 11.45 nm.

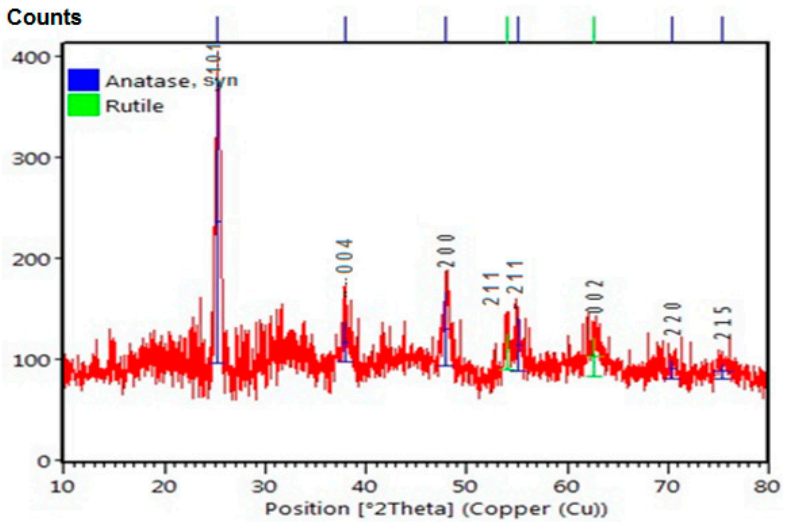

Figure 2. XRD pattern of TiO_2 NPs.

Table 1. The structural and geometrical parameters of TiO_2 NPs.

Sr No.	Peak Position 2θ (Degree)	FWHM Left [9]	Lattice Planes (h k l)	Inter-Planar Distance d Spacing (nm)	Crystallite Size D (nm)
1	25.295	0.56	101	3.51812	14.44
2	37.98	0.85	004	2.36692	9.82
3	47.98	0.76	200	1.89456	11.36
4	53.99	0.52	211	1.69713	17.13
5	55.02	0.6	211	1.66753	15.42
6	62.65	2.0	002	1.48155	4.62
7	70.43	0.7	220	1.33585	13.88
8	75.3	2	215	1.26074	4.98

3.3. Fourier Transforms Infrared (FT-IR) Spectroscopy

The functional groups and chemical bonds present in the TiO_2 NPs were determined by FT-IR spectroscopy. The FT–IR spectrum of the TiO_2 NPs is shown in Figure 3. The broad band at 3709–3712 cm^{-1} corresponds to O–H stretching vibrations. The bending vibration of functional groups C–H is reflected in the band between 1513 and 1516 cm^{-1} [2]. Below 1200 cm^{-1}, the characteristic absorption band of green-synthesized TiO_2 NPs was observed. The Ti–O–Ti vibrations are primarily responsible for this distinctive absorption peak [1]. The peak at around 3000 cm^{-1} was the result of –OH stretching [8]. The spectrum also shows peaks at 1365 cm^{-1} for nitro compounds, 1544 cm^{-1} for amide–II from proteins, 1642 cm^{-1} for H–O–H bending vibrations, and 1796–1725 cm^{-1} for carbonyl (polyol) esters [11]. Table 2 displays the tentative frequency and band assignments. These particles have various natural functional groups which append to the outer layer of TTIP, causing a decrease in exposed TTIP. As a result, they serve as both capping agents and reducing agents.

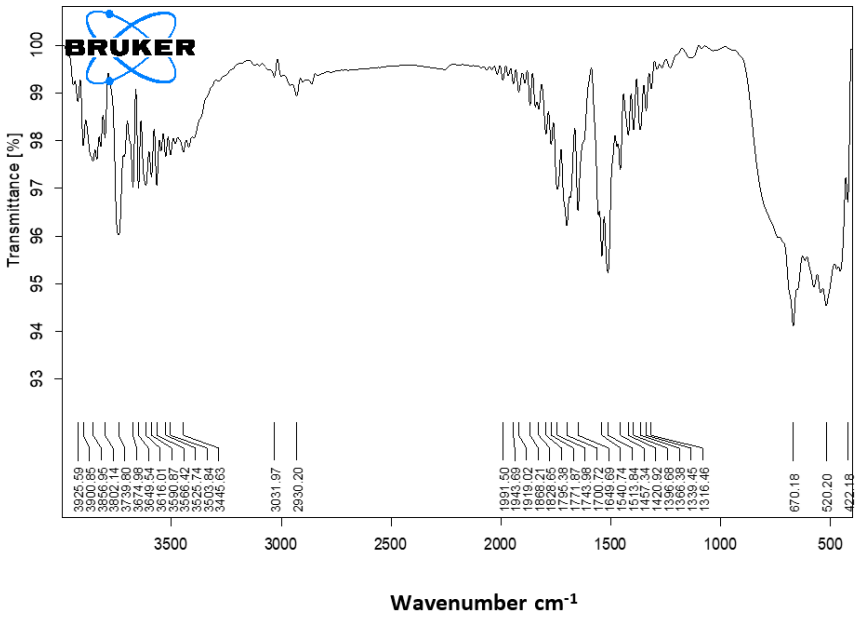

Figure 3. FT–IR spectrum of TiO_2 NPs.

Table 2. FT-IR analysis of TiO_2 NPs.

S.NO	Wave Number (cm^{-1})	Band Assignment
1	3709–3712 cm^{-1}	O–H stretching vibration
2	3000 cm^{-1}	–OH stretching
3	1796–1725 cm^{-1}	carbonyl (polyol' s) esters
4	1642 cm^{-1}	H–O–H bending vibrations
6	1544 cm^{-1}	amide–II from proteins
7	1513–1516 cm^{-1}	bending vibration of functional groups C–H
8	1365 cm^{-1}	nitro compounds
9	below 1200 cm^{-1}	Ti–O and Ti–O–Ti bending vibrations

3.4. Dynamic Light Scattering (DLS) Analysis

The hydrodynamic diameter of the biosynthesized TiO_2 NPs was determined using particle size analysis. The mean particle size of the biosynthesized TiO_2 NPs was estimated to be 129.68 nm. Figure 4 shows the particle size distribution curve for the biosynthesized TiO_2 NPs.

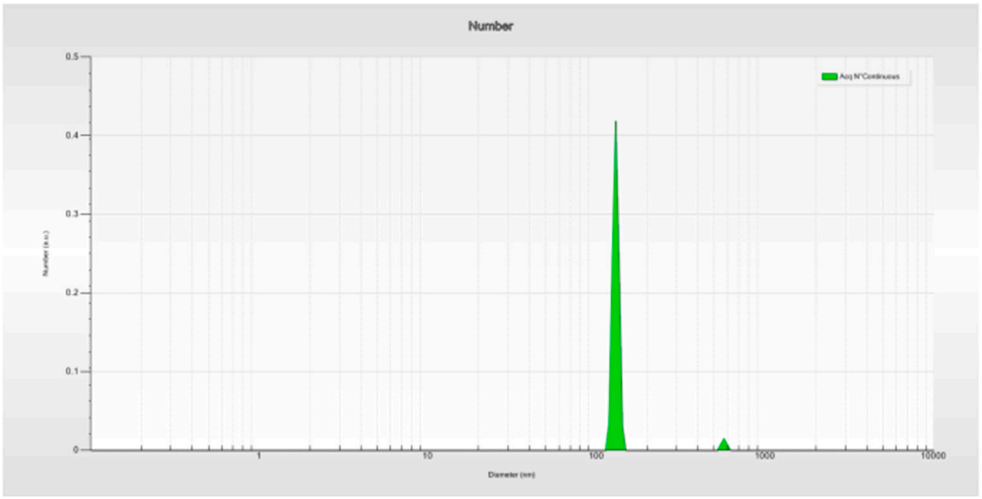

Figure 4. DLS analysis.

3.5. Field Emission Scanning Electron Microscopy (FE-SEM) Images

The surface morphology of the NPs and histogram of their particle size distribution are shown in Figure 5. The SEM images showed the spherical shape of the TiO_2 NPs, which was particularly evident at higher magnifications. It has been suggested that excess H^+ ions from H_2O molecules on the surface of the TiO_2 NPs could be the cause of the observed aggregation. Through van der Waals forces, these ions reduce the repulsion between the TiO_2 molecules [11]. EDAX analysis was used to conduct a compositional analysis of the synthesized TiO_2 NPs. As shown in Figure 5b, the NPs contained 61.51 percent by weight of Ti, 34.89 percent oxygen, 2.73 percent potassium, and 0.87 percent carbon. The presence of TiO_2 NPs is confirmed by this. The presence of biomolecules in the extract of *J. regia* green husk is the cause of the observed C and K peaks [12]. The histogram of the particle size distribution of the TiO_2 NPs is shown in Figure 5c.

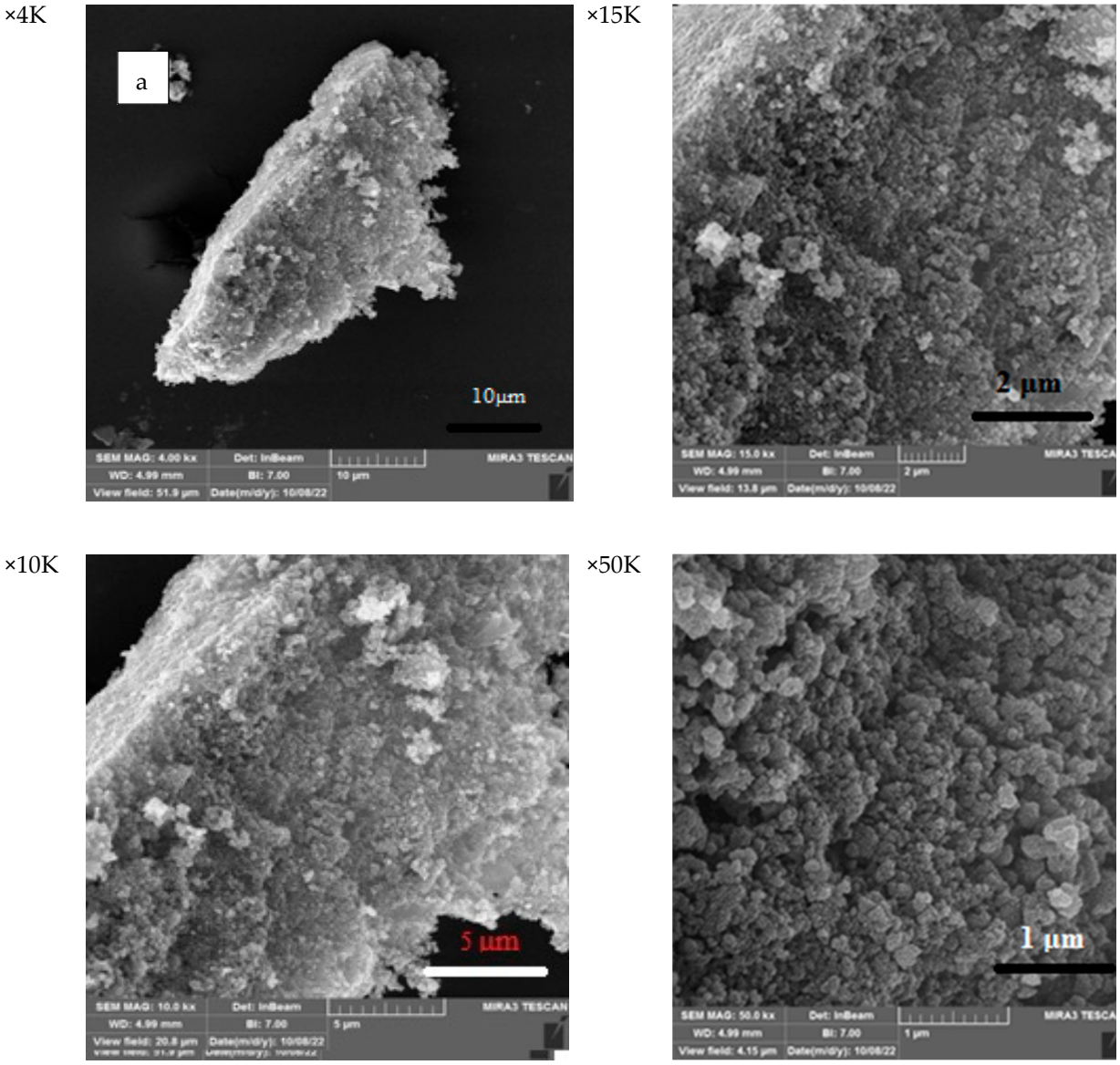

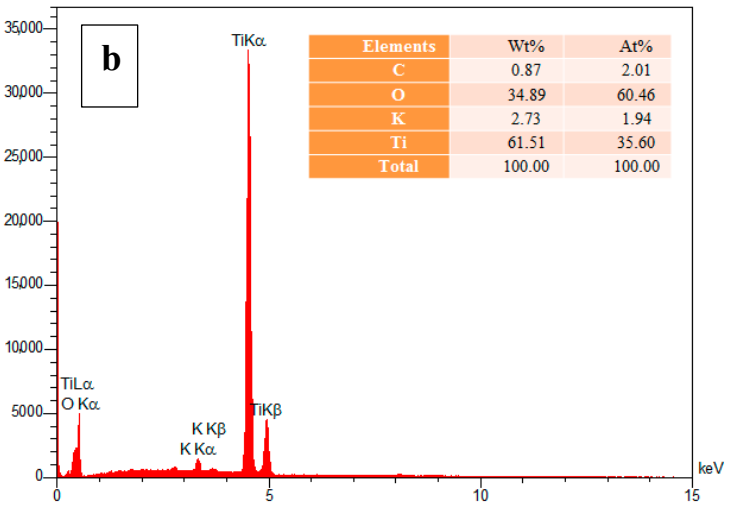

Elements	Wt%	At%
C	0.87	2.01
O	34.89	60.46
K	2.73	1.94
Ti	61.51	35.60
Total	100.00	100.00

Figure 5. *Cont.*

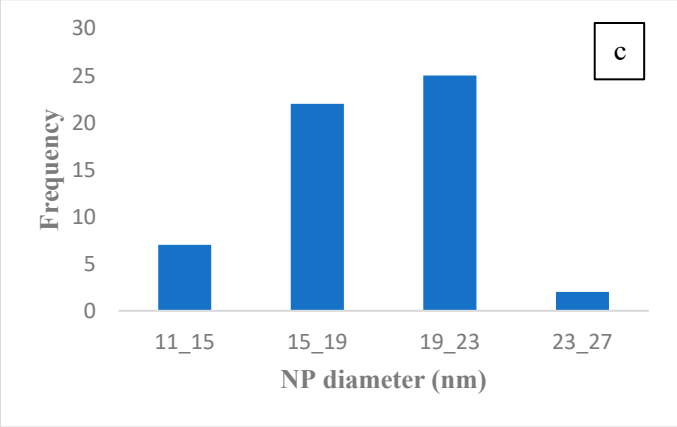

Figure 5. (**a**) FE-SEM images and (**b**) EDX image of synthesized TiO_2 NPs, and (**c**) Histogram of TiO_2 NP size distribution.

4. Conclusions

The synthesis of TiO_2 NPs using *J. regia* green husk aqueous extract was successfully carried out using the biosynthesis method. UV–Vis Spectroscopy, XRD, FT-IR, DLS, and FE-SEM were used to examine the optical and structural properties of the synthesized NPs. The XRD, DLS, and SEM results revealed that the two distinct polymorphs of TiO_2 NPs had spherical morphology and an average diameter of 19–23 nm. The calculated energy band gap of the synthesized TiO_2 NPs was 3.67 eV, which was greater than the band gap of bulk TiO_2 (3.2 eV). The role of the leaf extract in the TiO_2 NP synthesis was determined by FT-IR analysis. The current study demonstrates that the novel biosynthesis of TiO_2 NPs using *J. regia* aqueous extract of the green husk is possible and involves inexpensive precursors. This easy, cost-effective, and green synthesis method is useful for a variety of applications.

Author Contributions: Z.H. performed the study, analyzed the data and wrote the original draft. P.G. conceived, proposed and designed the study and also as corresponding author, sponsored the study, and made all the arrangements. All authors reviewed and edited the final version of the manuscript. All authors have read and agreed to the published version of the manuscript.

Funding: This research received no external funding.

Institutional Review Board Statement: Not applicable.

Informed Consent Statement: Not applicable.

Data Availability Statement: Not applicable.

Acknowledgments: This study was financially supported by the research council of Alzahra University, Tehran, Iran.

Conflicts of Interest: The authors declare no conflict of interest.

References

1. Ahmad, W.; Jaiswal, K.K.; Soni, S. Green synthesis of titanium dioxide (TiO_2) nanoparticles by using Mentha arvensis leaves extract and its antimicrobial properties. *Inorg. Nano-Met. Chem.* **2020**, *50*, 1032–1038. [CrossRef]
2. Aravind, M.; Amalanathan, M.; Mary, M.S.M. Synthesis of TiO_2 nanoparticles by chemical and green synthesis methods and their multifaceted properties. *SN Appl. Sci.* **2021**, *3*, 409. [CrossRef]
3. Patidar, V.; Jain, P. Green synthesis of TiO_2 nanoparticle using Moringa oleifera leaf extract. *Int. Res. J. Eng. Technol.* **2017**, *4*, 1–4.
4. Keat, C.L.; Aziz, A.; Eid, A.M.; Elmarzugi, N.A. Biosynthesis of nanoparticles and silver nanoparticles. *Bioresour. Bioprocess.* **2015**, *2*, 47. [CrossRef]
5. Muniandy, S.S.; Kaus, N.H.M.; Jiang, Z.-T.; Altarawneh, M.; Lee, H.L. Green synthesis of mesoporous anatase TiO_2 nanoparticles and their photocatalytic activities. *RSC Adv.* **2017**, *7*, 48083–48094. [CrossRef]
6. Ahn, E.-Y.; Shin, S.-W.; Kim, K.; Park, Y. Facile green synthesis of titanium dioxide nanoparticles by upcycling mangosteen (Garcinia mangostana) pericarp extract. *Nanoscale Res. Lett.* **2022**, *17*, 40. [CrossRef] [PubMed]

7. Hunagund, S.M.; Desai, V.R.; Barretto, D.A.; Pujar, M.S.; Kadadevarmath, J.S.; Vootla, S.; Sidarai, A.H. Photocatalysis effect of a novel green synthesis gadolinium doped titanium dioxide nanoparticles on their biological activities. *J. Photochem. Photobiol. A Chem.* **2017**, *346*, 159–167. [CrossRef]
8. Mathew, S.S.; Sunny, N.E.; Shanmugam, V. Green synthesis of anatase titanium dioxide nanoparticles using Cuminum cyminum seed extract; effect on Mung bean (Vigna radiata) seed germination. *Inorg. Chem. Commun.* **2021**, *126*, 108485. [CrossRef]
9. Gupta, K.; Singh, R.; Pandey, A.; Pandey, A. Correction: Photocatalytic antibacterial performance of TiO_2 and Ag-doped TiO_2 against S. aureus. P. aeruginosa and *E. coli*. *Beilstein J. Nanotechnol.* **2020**, *11*, 547–549. [CrossRef] [PubMed]
10. Jenkins, R.; Snyder, R.L. *Introduction to X-ray Powder Diffractometry (Volume 138)*; Wiley Online Library: Hoboken, NJ, USA, 1996.
11. Kaur, H.; Kaur, S.; Singh, J.; Rawat, M.; Kumar, S. Expanding horizon: Green synthesis of TiO_2 nanoparticles using Carica papaya leaves for photocatalysis application. *Mater. Res. Express* **2019**, *6*, 095034. [CrossRef]
12. Abbasi, Z.; Feizi, S.; Taghipour, E.; Ghadam, P. Green synthesis of silver nanoparticles using aqueous extract of dried Juglans regia green husk and examination of its biological properties. *Green Process. Synth.* **2017**, *6*, 477–485. [CrossRef]